Small-angle Neutron Scattering from Mixtures of Long- and Short-chain 3-Alkyl-1-methyl Imidazolium Bistriflimides

Christopher P. Cabry[a], Lucia D'Andrea[a], Naomi S. Elstone,[a]

Sarah Kirchhecker[a], Iman Khazal[a], Peixun Li[b], Sarah Rogers[b],

Duncan W. Bruce[a],* and John M. Slattery[a],*

[a] Department of Chemistry
University of York
Heslington
YORK YO10 5DD (UK)
Tel: (+44) 1904 324085
E-mail: john.slattery@york.ac.uk, duncan.bruce@york.ac.uk

[b] ISIS
Science & Technology Facilities Council,
Rutherford Appleton Laboratory
Chilton
UK

Teubner-Strey Model: an empirical model that uses the scattering intensity, *I*, determined at scattering vector *q* according to:

$$I(q) = \frac{1}{a + c_1 q^2 + c_2 q^4} + \text{background}$$

Here, a, c_1 and c_2 are empirical fitting parameters which, in different combinations, yield the d-spacing, *correlation length* and *amphiphile strength* (γ) according to:

$$d\text{-spacing} = \frac{2\pi}{\sqrt{\frac{1}{2}\sqrt{\frac{a}{c_2}} - \frac{c_1}{4c_2}}} \qquad \text{correlation length} = \frac{1}{\sqrt{\frac{1}{2}\sqrt{\frac{a}{c_2}} + \frac{1}{4}\frac{c_1}{c_2}}}$$

$$\text{amphiphile strength} (\gamma) = \frac{c_1}{\sqrt{4ac_2}}$$

The *d*-spacing relates to the periodic distance in a lamellar or bicontinuous structure or, where such structures do not exist, it relates to the average distance between scattering objects. The correlation length relates to the length scale of the scattering objects, while γ describes the type of structure formed by the system according to one of four ranges:

$\gamma > 1$ – system regarded as disordered
$1 > \gamma > 0$ – aggregates/micelles exist
$0 > \gamma > -1$ – percolated/bicontinuous structure exists
$-1 > \gamma$ - lamellar structure exists.

In cases where the Teubner-Strey model could not describe the observed scattering, Lorentz and Peak Lorentz Models were found useful in describing broad scattering features at low (Lorentz model) and high (peak Lorentz) values of *q*.

Lorentz + Peak Lorentz Model: These two models were used where the Teubner-Strey model could not describe the observed scattering and were found useful in describing broad scattering features at low (Lorentz model) and high (peak Lorentz) values of *q*, which are features of the data

for the mixtures under study and are generally associated with a lack of order on longer lengthscales. The models are described by:

$$I(q) = \frac{\text{scale}}{\left(1+\left(qL\right)^2\right)} + \text{background} \qquad\qquad I(q) = \frac{\text{scale}}{\left(1+\left(\dfrac{q-q_0}{B}\right)^2\right)} + \text{background}$$

<div align="center">Lorentz   peak Lorentz</div>

In the former case, L is the correlation length, which has the same significance as in the Teubner-Strey model. In the latter model, a correlation length is calculated from $2\pi/q_0$ where q_0 is the centre position of a peak of height I_0 with HWHM = B.

Table S1: Mixtures and contrasts used in the present SANS studies.

Isotopic contrast	Compositions, x
$[C_2C_1im\text{-}d_{11}]_{1\text{-}x}[C_{12}C_1im]_x[Tf_2N]$ (C12-HH in C2-DD)	0, 0.01, 0.04, 0.16, 0.24, 0.32, 0.52, 0.74, 0.87, 0.96, 0.99, 1
$[C_2C_1im]_{1\text{-}x}[C_{12}C_1im\text{-}d_{31}]_x[Tf_2N]$ ((C12-DD in C2-HH))	0, 0.01, 0.04, 0.16, 0.24, 0.32, 0.52, 0.74, 0.87, 0.96, 0.99, 1
$C_2C_1im\text{-}d_{11}]_{1\text{-}x}[C_{10}C_1im]_x[Tf_2N]$ (C10-HH in C2-DD)	0, 0.01, 0.03, 0.12, 0.18, 0.25, 0.44, 0.65, 0.74, 0.84, 0.96, 0.99, 1
$[C_2C_1im]_{1\text{-}x}[C_{10}C_1im\text{-}d_{27}]_x[Tf_2N]$ ((C10-DD in C2-HH))	0, 0.01, 0.03, 0.12, 0.18, 0.25, 0.44, 0.65, 0.74, 0.84, 0.96, 0.99, 1
$[C_2C_1im\text{-}d_{11}]_{1\text{-}x}[C_8C_1im]_x[Tf_2N]$ ((C8-HH in C2-DD)	0, 0.01, 0.03, 0.12, 0.18, 0.25, 0.44, 0.67, 0.83, 0.95, 0.99, 1
$[[C_2C_1im]_{1\text{-}x}[C_8C_1im\text{-}d_{23}]_x[Tf_2N]$ (C8-DD in C2-HH)	0, 0.01, 0.03, 0.12, 0.18, 0.25, 0.44, 0.67, 0.83, 0.95, 0.99, 1
$[C_2C_1im\text{-}d_{11}]_{1\text{-}x}[C_6C_1im]_x[Tf_2N]$ (C6-HH in C2-DD)	0, 0.01, 0.03, 0.13, 0.19, 0.27, 0.46, 0.69, 0.84, 0.95, 0.99, 1
$[C_2C_1im]_{1\text{-}x}[C_6C_1im\text{-}d_{19}]_x[Tf_2N]$ (C6-DD in C2-HH)	0, 0.02, 0.03, 0.13, 0.19, 0.27, 0.46, 0.69, 0.84, 0.95, 0.99, 1
$[C_2C_1im\text{-}d_{11}]_{1\text{-}x}[C_4C_1im]_x[Tf_2N]$ (C4-HH in C2-DD)	0, 0.01, 0.03, 0.14, 0.21, 0.28, 0.48, 0.71, 0.85, 0.95, 0.99, 1
$[C_2C_1im]_{1\text{-}x}[C_4C_1im\text{-}d_{15}]_x[Tf_2N]$ (C4-DD in C2-HH)	0, 0.01, 0.03, 0.14, 0.21, 0.29, 0.44, 0.70, 0.85, 0.95, 0.99, 1

Table S2: Mixtures and contrasts used in the SANS studies with $[C_{12}C_1im][Tf_2N]$ and $[C_mC_1im][Tf_2N]$.

Isotopic contrast	Compositions
$[C_2C_1im\text{-}d_{11}]_{1-x}[C_{12}C_1im]_x[Tf_2N]$ (C12-HH in C2-DD)	x = 0, 0.01, 0.04, 0.16, 0.24, 0.32, 0.52, 0.74, 0.87, 0.96, 0.99, 1
$[C_2C_1im]_{1-x}[C_{12}C_1im\text{-}d_{31}]_x[Tf_2N]$ (C12-DD in C2-HH)	x = 0, 0.01, 0.04, 0.16, 0.24, 0.32, 0.52, 0.74, 0.87, 0.96, 0.99, 1
$[C_4C_1im\text{-}d_{15}]_{1-x}[C_{12}C_1im]_x[Tf_2N]$ (C12-HH in C4-DD)	x = 0, 0.01, 0.04, 0.16, 0.24, 0.32, 0.52, 0.74, 0.87, 0.96, 0.99, 1
$[C_4C_1im]_{1-x}[C_{12}C_1im\text{-}d_{31}]_x[Tf_2N]$ (C12-DD in C4-HH)	x = 0, 0.01, 0.04, 0.16, 0.24, 0.32, 0.52, 0.74, 0.87, 0.96, 0.99, 1
$[C_6C_1im\text{-}d_{19}]_{1-x}[C_{12}C_1im]_x[Tf_2N]$ (C12-HH in C6-DD)	x = 0, 0.01, 0.04, 0.16, 0.24, 0.32, 0.52, 0.74, 0.87, 0.96, 0.99, 1
$[[C_8C_1im]_{1-x}[C_{12}C_1im\text{-}d_{31}]_x[Tf_2N]$ (C12-DD in C6-HH)	x = 0, 0.01, 0.04, 0.16, 0.24, 0.32, 0.52, 0.67, 0.74, 0.87, 0.96, 0.99, 1
$[C_2C_1im\text{-}d_{11}]_{1-x}[C_{12}C_1im]_x[Tf_2N]$ (C12-HH in C8-DD)	x = 0, 0.01, 0.04, 0.16, 0.24, 0.32, 0.52, 0.67, 0.74, 0.87, 0.96, 0.99, 1
$[C_2C_1im]_{1-x}[C_{12}C_1im\text{-}d_{31}]_x[Tf_2N]$ (C12-DD in C8-HH)	0, 0.01, 0.04, 0.16, 0.24, 0.32, 0.52, 0.67, 0.74, 0.87, 0.96, 0.99, 1

Table S3 Parameters relating to the fitting of data for mixtures $[C_4mim]_x[C_2mim\text{-}d_{11}]_{1\text{-}x}[Tf_2N]$ and $[C_4mim\text{-}d_{15}]_x[C_2mim]_{1\text{-}x}[Tf_2N]$

| Sample	Radius / Å	SLD x 10⁻⁶ Å⁻²	SLD bulk x 10⁻⁶ Å⁻²	Scale	Background
1% C4DD in C2HH	6.81 ± 0.13	9.7	2.4	0.006 ± 0.0004	0.017 ± 0.0005
1% C4HH in C2DD	-	-	5.0	-	-
4% C4DD in C2HH	6.78 ± 0.10	9.7	2.5	0.008 ± 0.0003	0.015 ± 0.0004
4% C4HH in C2DD	8.72 ± 0.42	1.0	4.9	0.003 ± 0.0004	0.006 ± 0.0004
16% C4DD in C2HH	6.16 ± 0.07	9.7	2.9	0.017 ± 0.0007	0.029 ± 0.0005
16% C4HH in C2DD	6.64 ± 0.07	1.0	4.6	0.03 ± 0.001	0.004 ± 0.0002
24% C4DD in C2HH	6.47 ± 0.07	9.7	3.2	0.013 ± 0.0003	0.003 ± 0.0003
24% C4HH in C2DD	6.04 ± 0.05	1.0	4.3	0.06 ±0.002	0.005 ± 0.0003
32% C4DD in C2HH	5.72 ± 0.04	9.7	3.4	0.031 ± 0.0004	0.016 ± 0.0004
32% C4HH in C2DD	5.85 ± 0.04	1.0	4.1	0.10 ± 0.002	0.005 ± 0.0003
52% C4DD in C2HH	5.53 ± 0.03	9.7	4.0	0.045 ± 0.0007	0.014 ± 0.0003
54% C4HH in C2DD	5.65 ± 0.04	1.0	3.4	0.22 ± 0.005	0.009 ± 0.0004
74% C4DD in C2HH	5.58 ± 0.06	9.7	4.7	0.038 ± 0.0008	0.029 ± 0.0003
74% C4HH in C2DD	5.55 ± 0.05	1.0	2.8	0.40 ± 0.010	0.009 ± 0.0004
87% C4DD in C2HH	7.06 ± 0.14	9.7	5.0	0.009 ± 0.0006	0.006 ±0.0004
87% C4HH in C2DD	5.91 ± 0.06	1.0	2.4	0.41 ± 0.014	0.006 ± 0.0004
96% C4DD in C2HH	10.80 ±0.77	9.7	5.2	0.0008 ± 0.0002	0.003 ± 0.0004
96% C4HH in C2DD	5.91 ± 0.06	1.0	2.2	0.35 ± 0.017	0.010 ± 0.0004
99% C4DD in C2HH	-	9.7	5.3	-	-
99% C4HH in C2DD	6.58 ± 0.12	1.0	2.1	0.31 ± 0.016	0.012 ± 0.0004
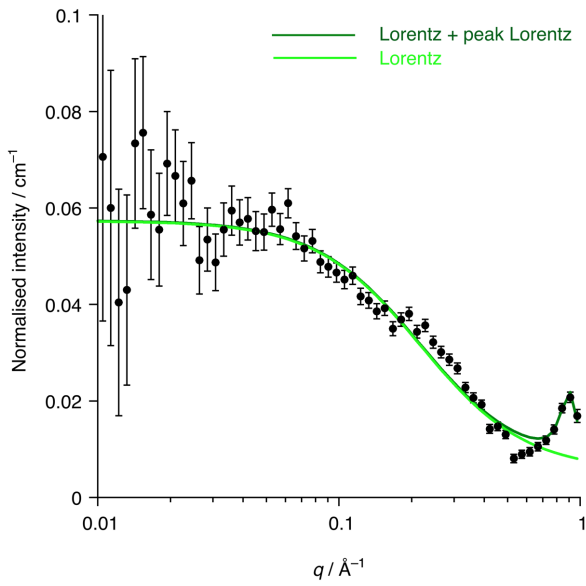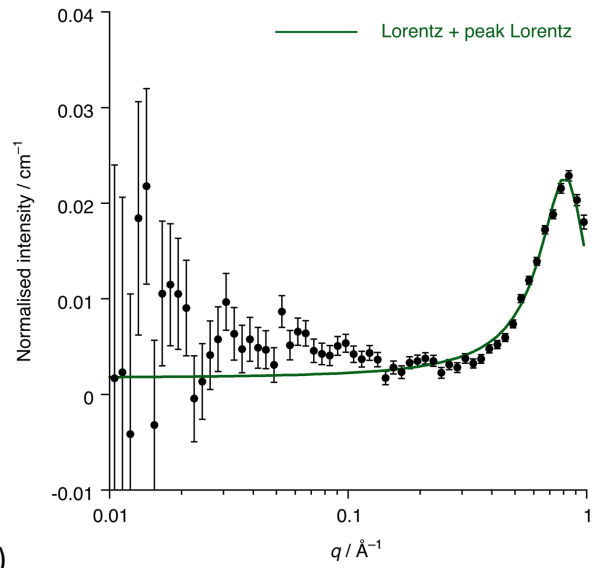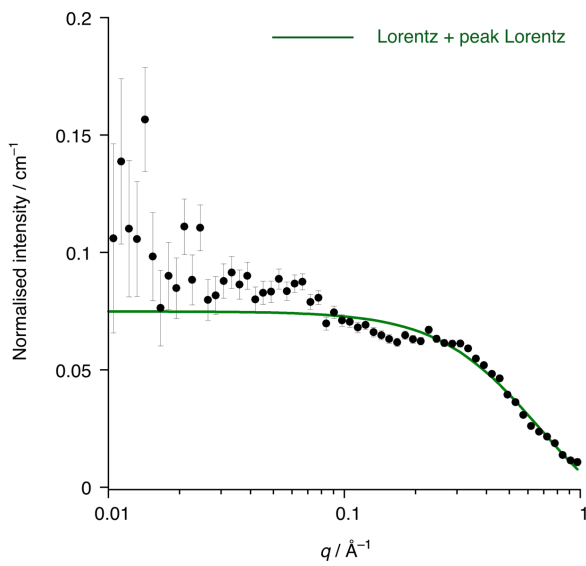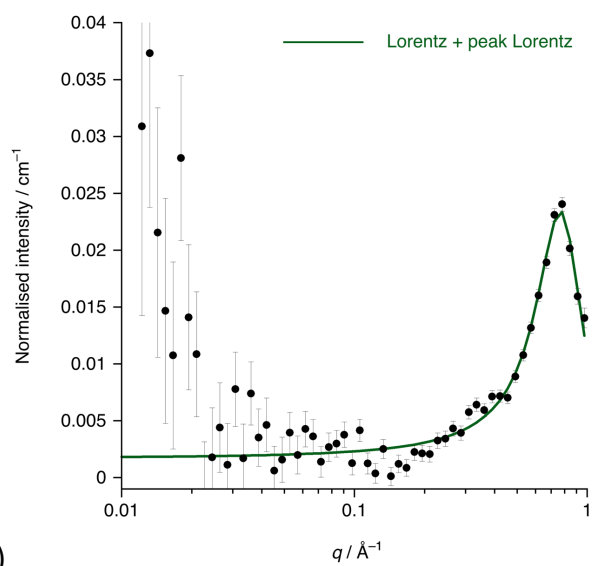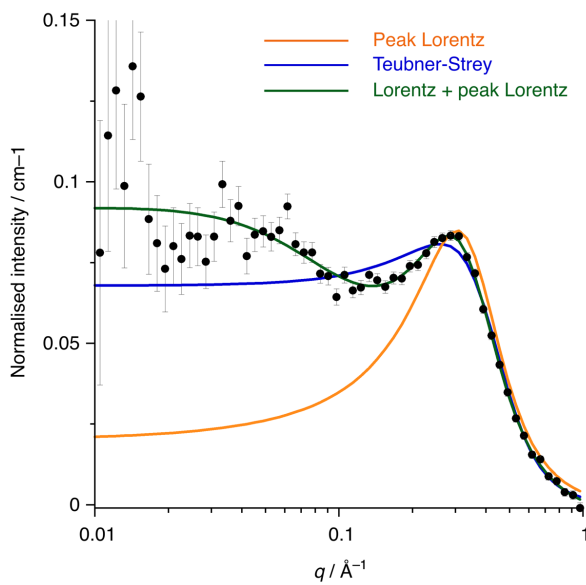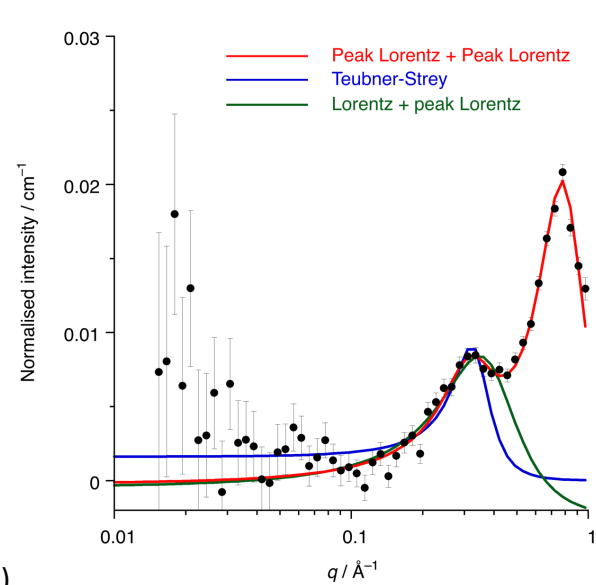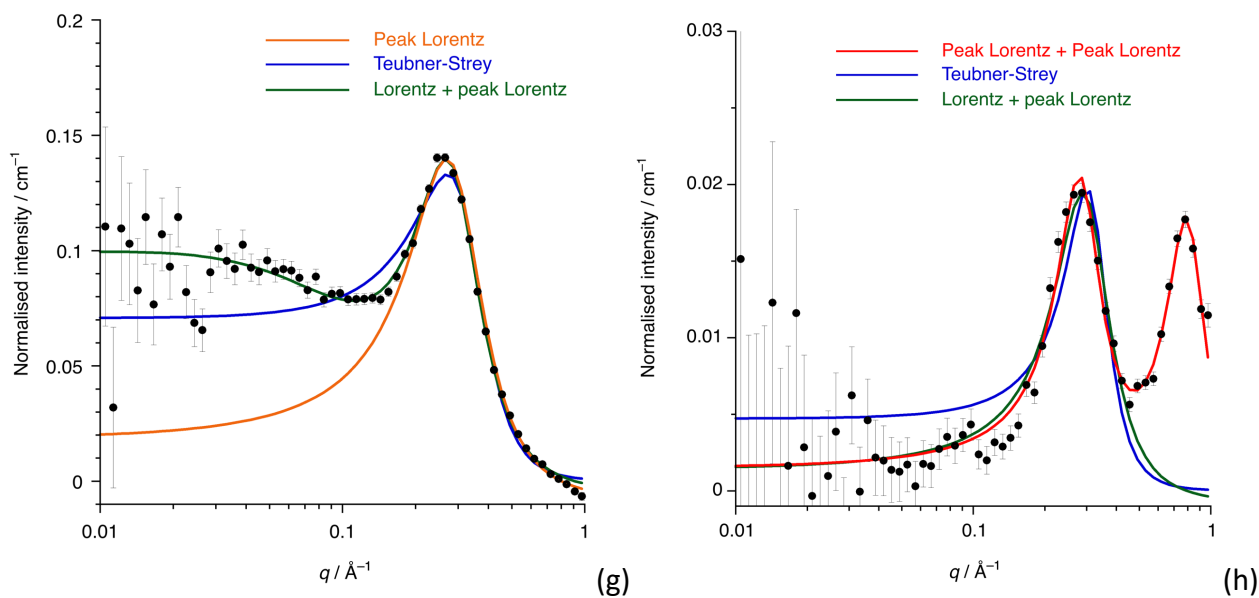
Figure S1: Fits to the SANS data for: (a) C2-HH; (b) C2-DD; (c) C6-HH; (d) C6-DD; (e) C8-HH; (f) C8-DD; (g) C10-HH and (h) C10-DD. Fitting models are indicated on each plot and all data are normalised to the background.
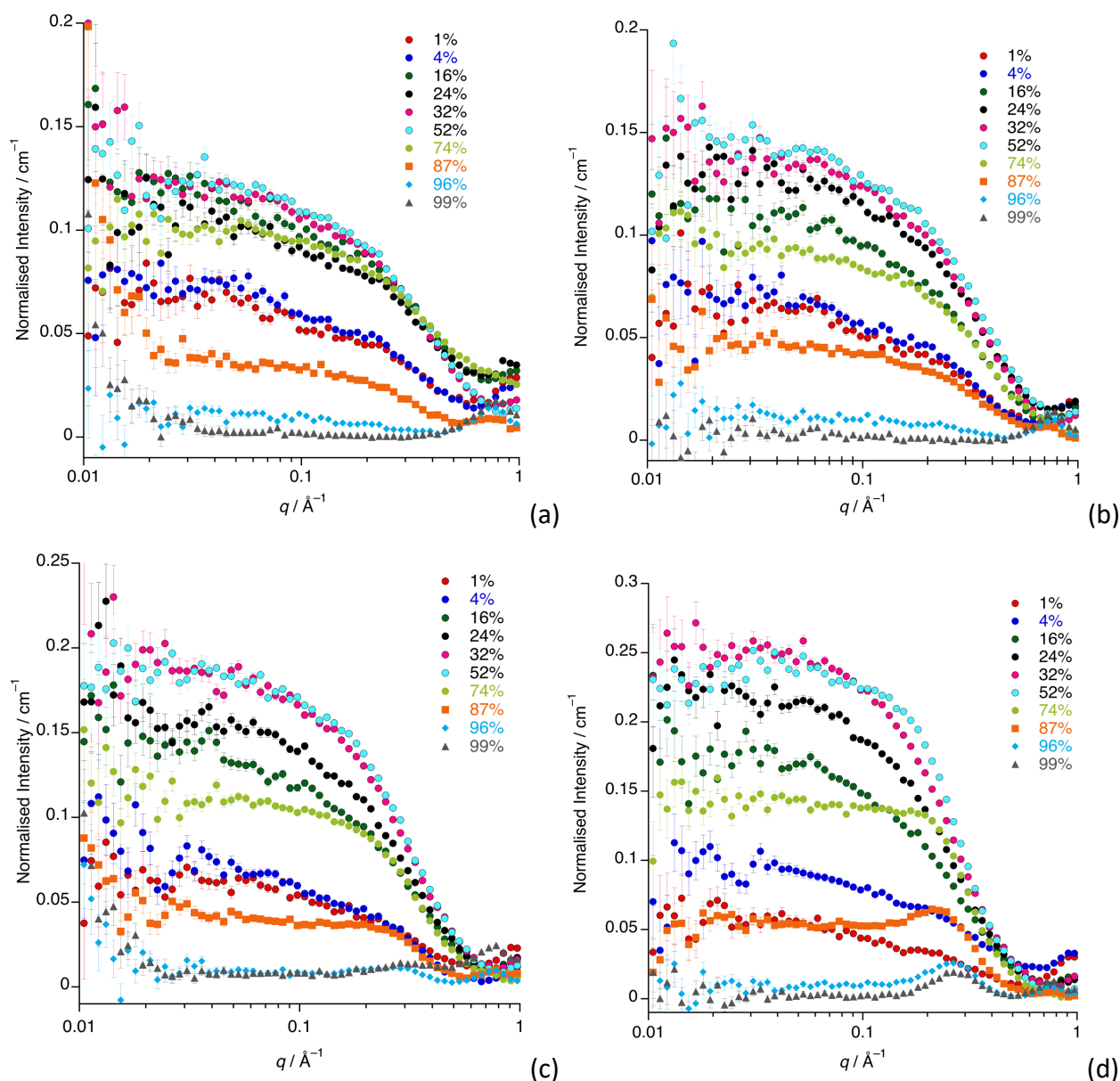
Figure S2: SANS data for mol fraction of: a) $[C_4mim\text{-}d_{15}][Tf_2N]$ in $[C_2mim][Tf_2N]$; b) $[C_6mim\text{-}d_{19}][Tf_2N]$ in $[C_2mim][Tf_2N]$; c) $[C_8mim\text{-}d_{23}][Tf_2N]$ in $[C_2mim][Tf_2N]$; d) $[C_{10}mim\text{-}d_{27}][Tf_2N]$ in $[C_2mim][Tf_2N]$. Data are normalised to the background.

Fitting Low-q Data for Mixtures of Composition $[C2\text{-}mim\text{-}d_{11}]_{1\text{-}x}[C4\text{-}mim]_x[Tf_2N]$

In order to fit these data efficiently, we have assumed that the SLD of the scattering object is equal to that calculated for $[C_4mim]^+$ and the bulk SLD is that of the average of all components present in the mixtures.

The variation in the intensity of the scattering from the different samples can be accounted for by the difference in the SLD of bulk versus scattering object decreasing as the concentration of $[C_4mim]^+$ increases while the number of scattering objects also increases, leading to an initial increase in scattering followed by a decrease as the SLD difference between the scattering objects and the bulk decreases. For some samples the fitting was complicated by the presence of peaks at high q, which are expected for these samples. The variation in the fitted radius may be due either to the scattering being from different components in the system or from variations within the orientation of the $[C_4mim]^+$ cation within this system, in order to fully determine this further contrasts would be required. Fits are shown in Figure S3.
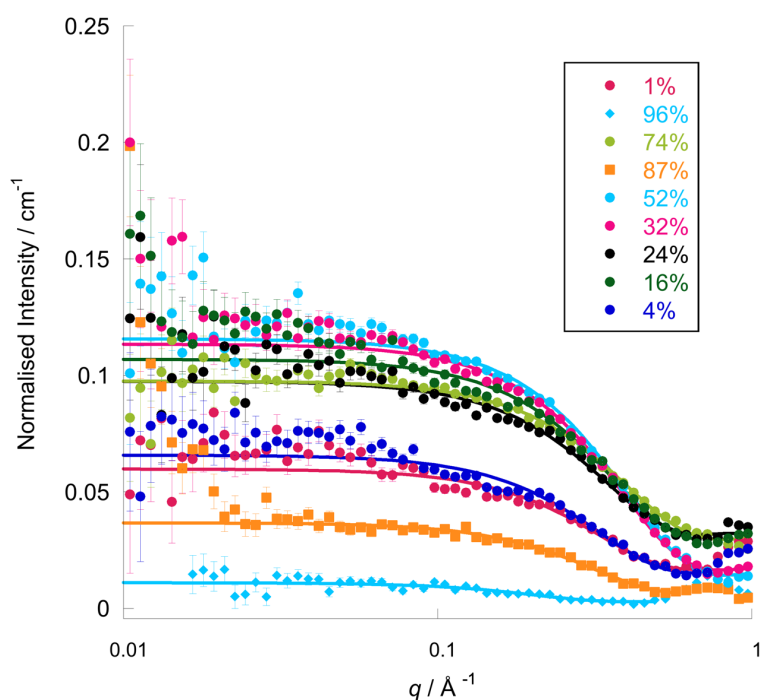

Figure S3 – Fitted data for the mixtures $[C2\text{-}mim\text{-}d_{11}]_{1-x}[C4\text{-}mim]_x[Tf_2N]$ (C4-HH in C2-DD) across the composition range.
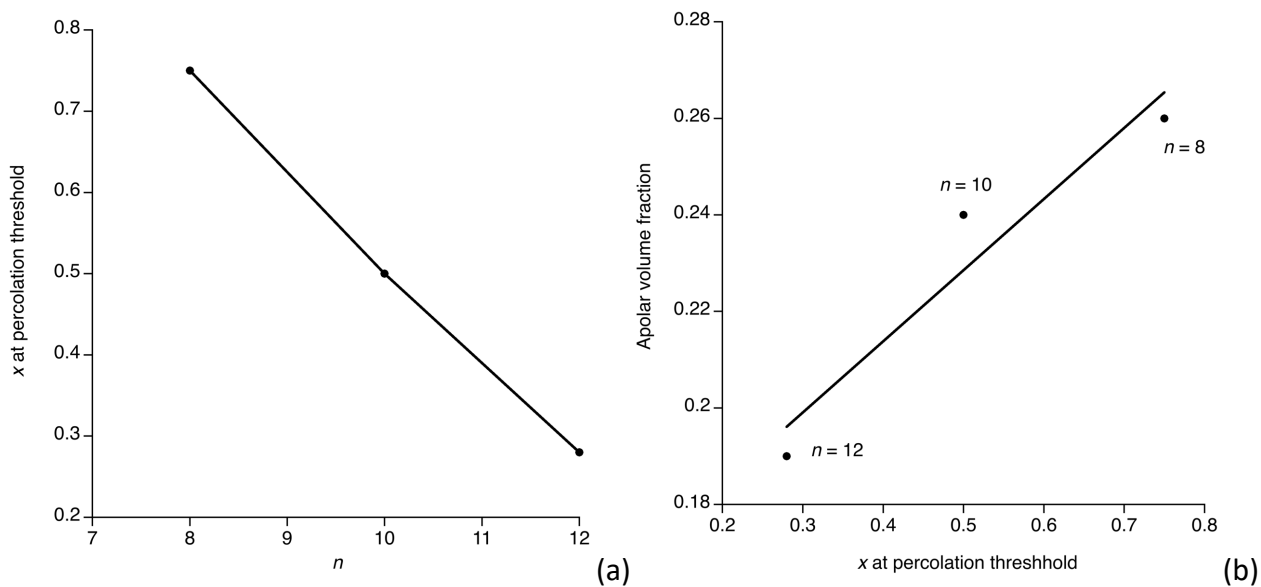
Figure S4: Linear regression analysis between (a) alkyl chain length n in the IL mixtures of $[C_2C_1im]_{x-1}[C_nC_1im]_x[Tf_2N]$ and the mole fraction (x) at which the percolation threshold is reached; (b) the mole fraction (x) at which the percolation threshold is reached in $[C_2C_1im]_{x-1}[C_nC_1im]_x[Tf_2N]$ IL mixtures with the apolar mole fraction of the liquids.
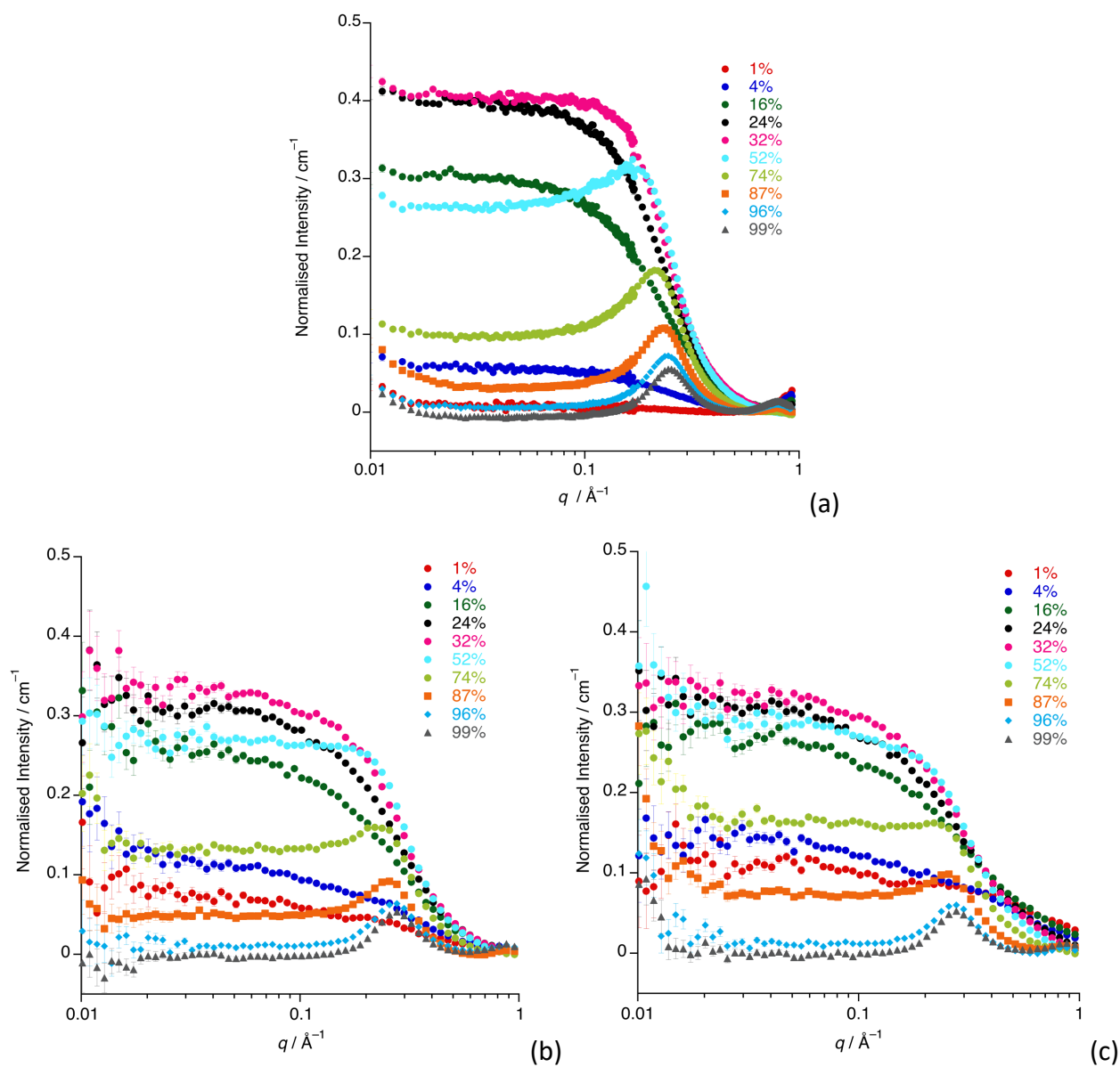
Figure S5 SANS data for: a) [C$_2$mim]$_{1-x}$[C$_{12}$mim-d$_{31}$]$_x$[Tf$_2$N]; b) [C$_4$mim]$_{1-x}$[C$_{12}$mim-d$_{31}$]$_x$[Tf$_2$N]; c) [C$_6$mim]$_{1-x}$[C$_{12}$mim-d$_{31}$]$_x$[Tf$_2$N]. All the data are normalised to the background.

(a)

(b)
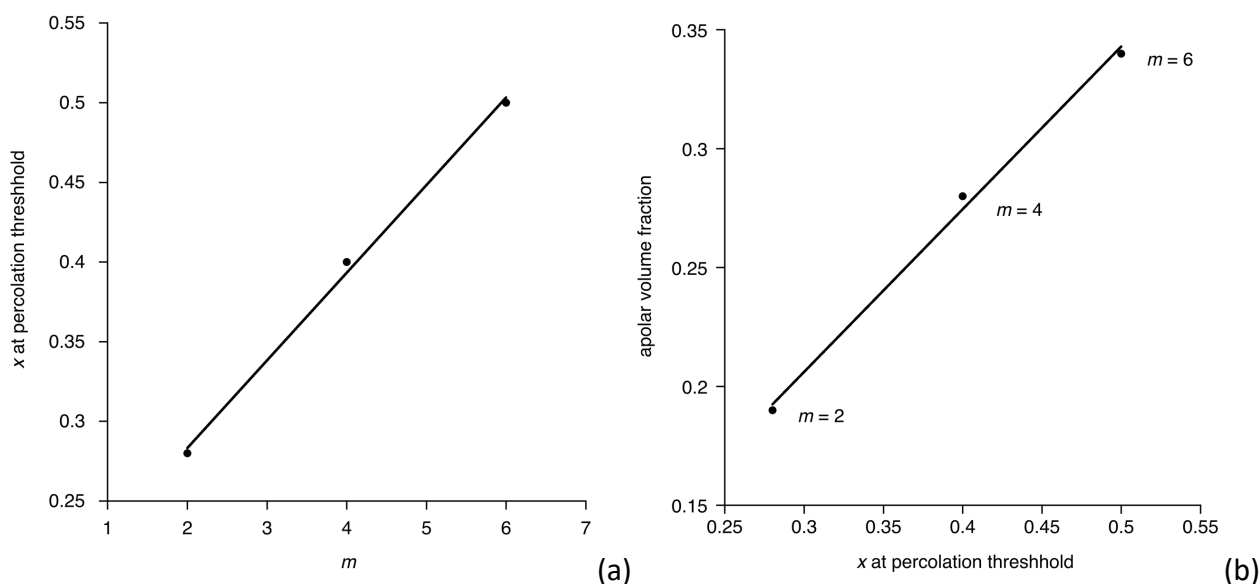
Figure S6 (a) Linear regression analysis between alkyl chain length m in the IL mixtures of $[C_mC_1im]_{x-1}[C_{12}C_1im]_x[Tf_2N]$ and the mole fraction (x) at which the percolation threshold is reached; (b) linear regression analysis between the mole fraction (x) at which the percolation threshold is reached in $[C_mC_1im]_{x-1}[C_{12}C_1im]_x[Tf_2N]$ IL mixtures with the apolar mole fraction of the liquids.
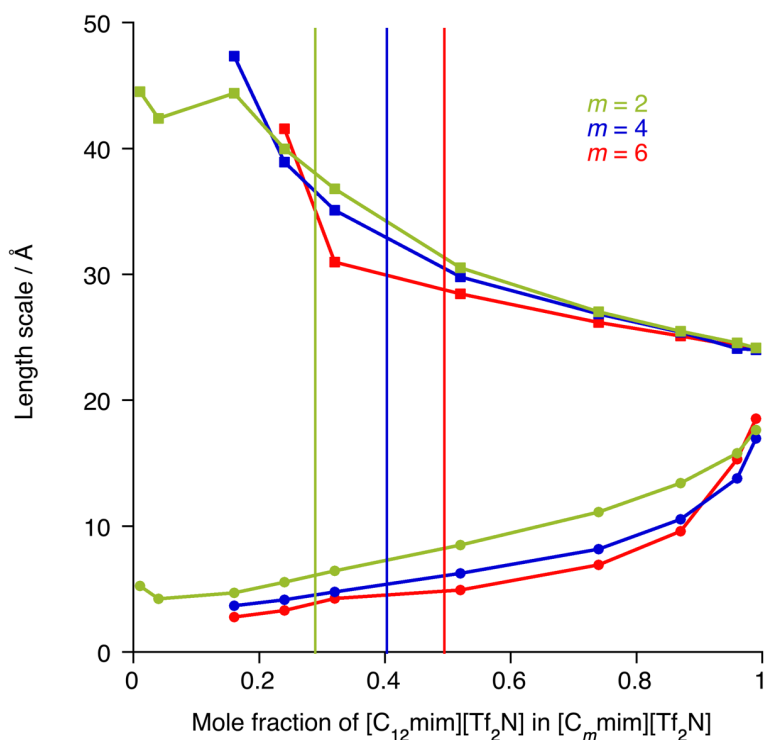

Figure S7 The length scale parameters from the Teubner-Strey model for the mixtures $[C_mC_1im\text{-}d_{2m+7}]_{1-x}[C_{12}C_1im]_x[Tf_2N]$. Squares represent the d-spacing, while circles represent the correlation length (ζ). The data are averaged values for the $[C_mC_1im\text{-}d_{2m+7}]_{1-x}[C_{12}C_1im]_x[Tf_2N]$ and $[C_mC_1im]_{1-x}[C_{12}C_1im\text{-}d_{31}]_x[Tf_2N]$ contrasts, where m = 6, 4, 2. The red, blue and olive vertical lines represent the mole fraction where the Lifshitz line is crossed for n = 6, 4, and 2 respectively.
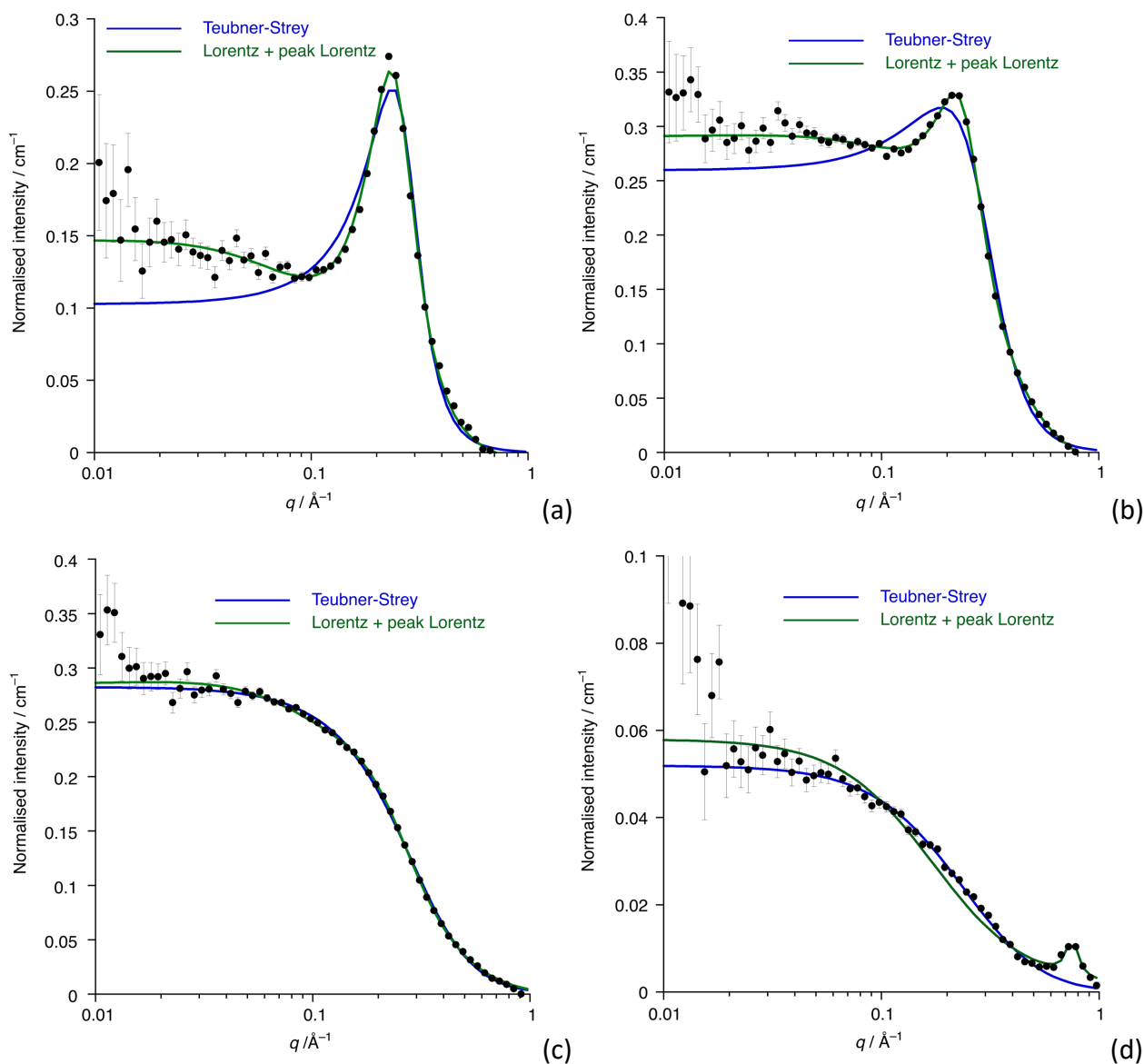
Figure S8 Fits to the Teubner-Strey (TS) model and Lorentz + peak Lorentz (L+PL) for $[C_8mm\text{-}d_{23}]_{1-x}[C_{12}mm]_x[Tf_2N]$ where x = (a) 0.96; b) 0.74; c) 0.24 and d) 0.04. The PL component of the L+PL model was used to model the data below $q \sim 0.4$ Å^{-1}, except for x = 0.04 where the PL component was used to model the COP.

Synthesis

Reagents and solvents were obtained from Sigma-Aldrich or Alfa Aesar and used without further purification, unless otherwise stated.

All air-sensitive experimental procedures were performed under an inert atmosphere of nitrogen using standard Schlenk line and glovebox techniques.

Toluene was purified using an Innovative Technologies anhydrous solvent engineering system. Dichloromethane, acetonitrile and hexane were purified by distillation using calcium hydride (for dichloromethane and acetonitrile) and sodium (for hexane) as drying agents. 1-Methylimidazole and [D$_3$]-1-methylimidazole were dried over calcium hydride and distilled under reduced pressure (10^{-3} mbar). Purification of the non–deuterated bromoalkanes was performed by distillation immediately prior to use, in the presence of activated 4 Å molecular sieves under nitrogen (1-bromoethane) or under reduced pressure. Deuterium oxide (99.9% D), [D$_5$]-1-bromoethane (99.0% D), and [D$_1$]-methanol (99.0% D) were obtained from Aldrich and used without further purification. [D$_3$]-1-iodomethane (99+% D) was purchased from Acros and used as received. [D$_{25}$]-1-bromododecane was provided by the ISIS deuteration facility and used as received. [D3]-methyl iodide (99+% D) was purchased from Acros and used as received. [D$_{21}$]-1-bromodecane was provided by the ISIS deuteration facility and used as received. [D$_9$]-1-bromobutane (98.0% D) was purchased from Goss Scientific. [D$_5$]-1-bromoethane (99.0% D), [D$_{13}$]-1-bromohexane (98.0% D), and [D$_{17}$]-1-bromooctane (98.0% D) from Sigma Aldrich and used as received.

^{1}H and ^{13}C{^{1}H} NMR spectra were recorded on either a Jeol ECS400 or a Jeol ECX400 (400 MHz for ^{1}H NMR) or a Bruker AV500 (500 MHz for ^{1}H NMR) at 298 K.

**1-Ethyl-3-methylimidazolium bromide, [C$_2$mim]Br**
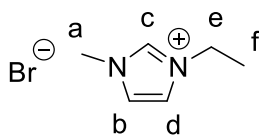
1-Ethyl-3-methylimidazolium bromide was prepared according to the literature method.[1] Distilled 1-methylimidazole (91.7 g, 89.0 cm^3, 1.12 mol) was added dropwise to an excess of freshly distilled 1-bromoethane (133.8 g, 92.0 cm^3, 1.23 mol). The mixture was stirred for 15 min at 50 °C, until the initial turbidity disappeared, and then for 2 h at 70 °C. Upon cooling to 0 °C, a white solid formed, which was ground in a glovebox. The solid was treated with ethyl acetate (20 cm^3) and

stirred at −10 °C for 1 h under nitrogen. After removing the solvent *via* cannula filtration, the white solid was dried under vacuum (10^{-2} mbar) at 60 °C for 6 h (185.7 g, 87%).

^{1}H NMR (400 MHz, DMSO-d_6, 293 K), δ (ppm): 9.29 (*s*, Hc, 1H), 7.87 (*m*, Hd, 1H), 7.78 (*m*, Hb, 1H), 4.24 (*q*, *J* = 7.3 Hz, He, 2H), 3.90 (*s*, Ha, 3H), 1.44 (*t*, *J* = 7.3 Hz, Hf, 3H).

All other homologues were prepared in an analogous manner noting that drying time varied between 4 and 7 d and also that [C$_{12}$mim]Br is a solid. Longer-chain homologues showed a broad resonance in the ^{1}H NMR spectrum corresponding to chain methylene hydrogens.

1-Ethyl-3-methylimidazolium bis(trifluoromethylsulfonyl)imide, [C$_2$mim][Tf$_2$N]
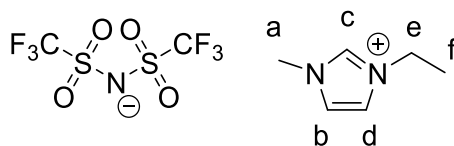

A solution of [C$_2$mim]Br (35.0 g, 0.18 mol) in deionised water (150 cm^3) was treated with a solution of LiTf$_2$N (53.2 g, 0.18 mol) in deionised water (150 cm^3). The biphasic system was stirred overnight at room temperature, under an atmosphere of nitrogen. An aqueous extraction (8 × 50 cm^3) was performed to remove the lithium halide until no precipitation of AgBr occurred in the aqueous phase upon addition of AgNO$_3$ solution. The colourless oil was then dried under vacuum (10^{-3} mbar) at 60 °C for 4 days (51.1 g, 71%).

^{1}H NMR (400 MHz, acetone-d_6). δ (ppm): 8.79 (s, Hc, 1H), 7.59 (s, Hd, 1H), 7.52 (s, Hb, 1H), 4.36 (q, *J* = 7.0 Hz, He, 2H), 4.02 (s, Ha, 3H), 1.63 (t, *J* = 7.0 Hz, Hf 3H).

All other homologues were prepared in an analogous manner. Longer-chain homologues showed a broad resonance in the ^{1}H NMR spectrum corresponding to chain methylene hydrogens.
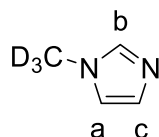
Sodium imidazolate
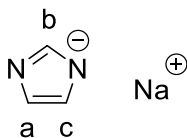
Deprotonation of imidazole was performed following a literature method with some modifications.[1] A suspension of sodium hydride (2.05 g, 85.4 mmol) in dry acetonitrile (150 cm^3) was cooled in an ice bath under a nitrogen atmosphere. Imidazole (5.53 g, 81.2 mmol) was ground into a fine powder and slowly added over a course of 3 h. A gentle effervescence of hydrogen occurred during addition. After 24 h of stirring, the solvent was removed under vacuum (10^{-1} mbar). Due to the hygroscopic nature of the product, the work-up was performed under nitrogen. The white solid was washed with dry hexane (4 × 30 cm^3) and dried at 100 °C under reduced pressure (10^{-1} mbar) for 1-2 h (6.93 g, 95%).

^{1}H NMR (400 MHz, D$_2$O). δ (ppm): 7.78 (s, Hb, 1H), 7.14 (s, Ha,c, 2H).
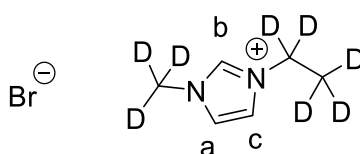
[D$_3$]-1-Methylimidazole

Methylation of sodium imidazolate was carried out following a literature method with some modifications.[1] Finely ground sodium imidazolate (28.00 g, 0.31 mol) was suspended in dry acetonitrile (350 cm^3) under nitrogen and cooled down in an ice/salt bath to −15 °C. To this, [D$_3$]-iodomethane (45.18 g, 19.4 cm^3, 0.31 mol) was added dropwise over a course of 3 h, during which time a yellow colour evolved. The resulting mixture was stirred at −15 °C for 3 − 5 additional h and then allowed to warm to room temperature. After 3 days of stirring, the solvent was removed under vacuum (10^{-1} mbar) to give an orange residue, which was then extracted with dry

dichloromethane (6 × 100 cm^3) *via* cannula transfer. A yellowish oil was obtained after removal of the dichloromethane under reduced pressure. The product was purified by vacuum distillation (10^{-1} mbar). The colourless liquid obtained (19.4 g, 73%) was stored at 4 °C under nitrogen. The degree of deuteration on the methyl group was quantitative.

^{1}H NMR (400 MHz, DMSO-d_6). δ (ppm): 7.60 (s, Hb,1H), 7.15 (s, Hc, 1H), 6.91 (s, Ha, 1H).

[D$_8$]-1-Ethyl-3-methylimidazolium bromide, [C$_2$C$_1$im-d_8]Br
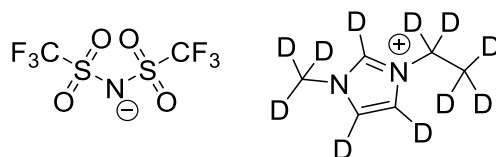

This product was prepared according to a literature method.[1,2] Distilled [D$_3$]-1-methylimidazole (3.92 g, 46.0 mmol) was added dropwise to a 10 mol% excess of [D$_5$]-bromoethane (5.70 g, 50.0 mmol). The mixture was stirred at room temperature for 20 min, 50 °C for 20 min, and then for 2 h at 70 °C. Upon cooling to room temperature, a white solid formed, which was ground under a blanket of ethyl acetate, followed by stirring in ethyl acetate at −10 °C for 1 h under nitrogen. After the solvent was removed *via* cannula filtration, the white solid was dried under vacuum (10^{-2} mbar) at room temperature for 2 h followed by 60 °C for 8 h (9.02 g, 98%). The degree of deuteration on the ethyl group was quantitative, as determined by ^{1}H NMR spectroscopy.

^{1}H NMR (400 MHz, acetone-d_6). δ (ppm): 10.08 (s, Hb, 1H), 7.86 (s, Hc, 1H), 7.77 (s, Ha, 1H).

Longer-chain homologues were prepared in an analogous fashion and gave the same ^{1}H NMR data. The bromide salts were then metathesised to the bistriflimides using the method outlined above for the protio analogues and were taken through to the next step without characterisation.

[D$_{11}$]-1-Ethyl-3-methylimidazolium bis(trifluoromethylsulfonyl)imide, [C$_2$C$_1$im-*d$_{11}$*][Tf$_2$N]

This product was prepared following a literature method.[1,2] [C$_2$C$_1$im-d$_8$][Tf$_2$N] (16.62 g, 41.5 mmol) was dissolved in [D$_1$]-methanol (102 cm^3), treated with caesium hydroxide monohydrate (2.05 g, 11.65 mmol) and stirred for 24 h at 50 °C under nitrogen. The mixture was neutralised with an 80% aqueous solution of bis(trifluoromethylsulfonyl)amide diluted 1:3 in D$_2$O, and the solvent was removed under vacuum (10^{-2} mbar). The residue was partitioned between dichloromethane and deuterium oxide. The layers were separated and the aqueous layer was extracted with dichloromethane. The combined organic layers were washed 3 times with deuterium oxide, and the solvent was removed under vacuum (10^{-2} mbar). The resulting colourless oil was dried under vacuum (10^{-3} mbar) at 60 °C for 6 h (16.09 g, 96%). The ^{1}H-NMR spectrum (CD$_2$Cl$_2$, 0.5 cm^3) of [C$_2$C$_1$im-*d$_{11}$*][Tf$_2$N] (47.9 mg, 0.119 mmol) in the presence of hexamethylbenzene (6.0 mg, 0.037 mmol) as an internal reference, revealed a degree of deuteration of 93% on the C2 position of the aromatic ring and 93% on the C4 and C5 positions.

Longer-chain analogues were prepared in an analogous manner.

Small-angle neutron scattering measurements

SANS was carried out on the Sans2d small-angle diffractometer at the ISIS Pulsed Neutron Source (STFC Rutherford Appleton Laboratory, Didcot, U.K.).[3] A simultaneous *q*-range of 0.0045 – 0.7 Å^{-1} was achieved utilising an incident wavelength range of 1.75 – 16.5 Å and employing an instrument set up of L1 = L2 = 4 m, with the 1 m^2 detector offset vertically 60 mm and sideways 100 mm. The beam diameter was 8 mm. Each raw scattering data set was corrected for the detector efficiencies, sample transmission and background scattering and converted to scattering cross-section data ($\delta\Sigma/\delta\Omega$ *vs q*) using the instrument-specific software.[4] These data were placed on an

absolute scale (cm^{-1}) using the scattering from a standard sample (a solid blend of hydrogenous and perdeuterated polystyrene) in accordance with established procedures.[5] The data were fitted using SasView software.[4]

References

1.   R. Giernoth and D. Bankmann, *Eur. J. Org. Chem.*, 2008, 2881-2886.

2.   D. W. Bruce, C. P. Cabry, J. N. C. Lopes, M. L. Costen, L. D'Andrea, I. Grillo, B. C. Marshall, K. G. McKendrick, T. K. Minton, S. M. Purcell, S. Rogers, J. M. Slattery, K. Shimizu, E. Smoll and M. A. Tesa-Serrate, *J. Phys. Chem. B*, 2017, **121**, 6002-6020.

3.   R. K. Heenan, S. E. Rogers, D. Turner, A. E. Terry, J. Treadgold and S. M. King, *Neutron News*, 2011, **22**, 19-21.

4.   www.sasview.org.

5.   G. D. Wignall and F. S. Bates, *J. Appl. Crystallogr.*, 1987, **20**, 28-40.